Inorganica Chimica Acta, 32 (1979) 209–215

PMR and ESR of Copper(II) Complexes Incorporating Pyrazine Analogs as Bridging Ligands

HIROYOSHI KURAMOTO and MOTOMICHI INOUE*
Department of Chemistry, Nagoya University, Nagoya 464, Japan
SHUJI EMORI and SHIGERU SUGIYAMA
Department of Chemistry, Saga University, Saga 840, Japan
Received June 9, 1978

PMR and ESR spectra were recorded on the crystal powders of pyrazine-2,3-dicarboxylatocopper-(II) and $Cu(NO_3)_2L$ type complexes (L: 2,5-dimethylpyrazine, 2,6-dimethylpyrazine, quinoxaline, chloropyrazine) at temperatures between 80 and 250 K. From the contact shifts in PMR, spin densities on the carbon atoms of the ligands were evaluated. A σ mechanism and three types of π mechanisms were proposed for the spin delocalization from copper to ligand molecules. The relative magnitude of the contributions from the mechanisms was estimated on the basis of the ESR results. The spin delocalization arises from the combined effect of the σ and π mechanisms, giving rise to antiferromagnetic interaction between copper atoms through the π systems of the bridging nitrogen heterocyclic ligands.

Introduction

A pyrazine complex with copper(II) nitrate, $Cu(NO_3)_2(paz)$, contains –Cu–(paz)–Cu– chains in crystals as shown in Fig. 1 [1]. The magnetic susceptibility can be explained well with Bonner–Fisher's [2] theoretical curve based on the linear Heisenberg model: antiferromagnetic interaction operates between copper atoms through bridging pyrazine molecules [3]. The magnetic susceptibilities of $Cu(NO_3)_2L$ type complexes incorporating pyrazine analogs as bridging ligands also can be interpreted with Bonner–Fisher's curve, suggesting the formation of –Cu–L–Cu– chains in crystals [4].

Matthews and Walton [5] prepared pyrazine-2,3-dicarboxylatocopper(II), $Cu(paz\cdot(COO)_2)$, and proposed a new type of polymeric structure as illustrated in Fig. 2 on the basis of the electronic and infrared spectra. The magnetic susceptibility obeys the Curie–Weiss law in the temperature range 80–300 K [5]. The Weiss constant equal to −4 K indicates that antiferromagnetic interaction operates between copper atoms almost to the same extent as in $Cu(NO_3)_2(paz)$, the Weiss constant of which is equal to −6 K [6].

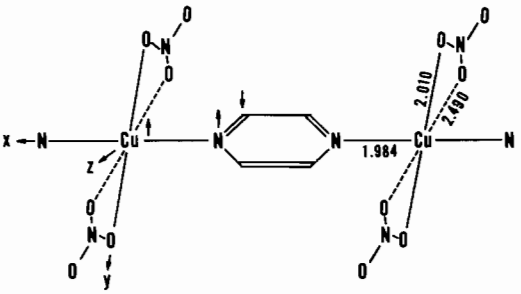

Figure 1. Linear chain in $Cu(NO_3)_2(paz)$. The arrows show the signs of spin densities.

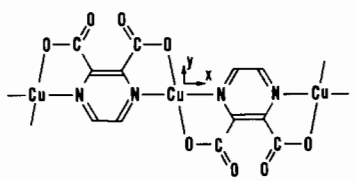

Figure 2. Proposed structure of pyrazine-2,3-dicarboxylatocopper(II).

These are good model compounds for studying superexchange interaction through bridging nitrogen heterocycles [7]. Superexchange mechanisms are closely related to spin delocalization from copper to bridging ligand molecules. This can be revealed by observing the Fermi contact shift in PMR spectra. For example, broad-line PMR studies of $Cu(NO_3)_2(paz)$ indicates that spin density amounting to −0.07– −0.08 is distributed on the carbon $p\pi$ orbitals of pyrazine, giving a direct experimental evidence for superexchange interaction operating through the π system of the ligand [6, 8]. This method is useful

*To whom correspondence should be addressed.

for getting information of superexchange mechanisms, because it can reveal the spin distribution of metal complexes in the crystalline states. Its application, however, is restricted to compounds containing only a few kinds of protons in crystals, because it is difficult, in a complex having various kinds of protons, to resolve the PMR absorption curve into component curves each attributable to one kind of equivalent protons. In the present investigation, the PMR technique has been applied to the crystal powders of $Cu(paz\cdot(COO)_2)$ and $Cu(NO_3)_2L$ complexes with 2,5-dimethylpyrazine (2,5-dmpaz), 2,6-dimethylpyrazine (2,6-dmpaz), chloropyrazine (Cl-paz), and quinoxaline (qux), each of which contains only a few kinds of protons in crystals. The spin-delocalization mechanism has been elucidated on the basis of the PMR results along with the results of ESR studies.

Experimental

$Cu(paz\cdot(COO)_2)$ was prepared by the method described by Matthews and Walton [5]. $Cu(NO_3)_2L$ complexes were prepared in the same way as $Cu(NO_3)_2(qux)$ [9]. The analytical value of copper of each compound agreed with the theoretical value within experimental error.

The broad-line PMR spectra of the crystal powders were recorded by means of a JEOL JNM-MW-40 NMR spectrometer operating at 40 MHz in the temperature range 78–250 K. Isohexane (isomeric mixture) was employed as an external standard. A magnetic field modulation of 280 Hz was used with an amplitude of 0.3–0.6 G (G: 10^{-4} T in the SI unit system), which is sufficiently smaller than the line width of the spectra. At liquid nitrogen temperature, no suitable external standard was available, and the modulation amplitude amounted to 1–2 G. For these reasons, the data obtained at one temperature involve a large uncertainty as compared with those at other temperatures. The temperature of the specimen was determined within 2° over the temperature range investigated by use of a copper–constantan thermometer, which was inserted directly in the specimen before and after recording each spectrum [10].

The ESR spectra of the powder crystals were recorded with a JEOL ES-SCXA X-band ESR spectrometer. The g factor was determined by recording simultaneously the signals of Mn^{2+}/MgO and DPPH employed as markers.

Results

PMR Spectrum of $Cu(paz\cdot(COO)_2)$

Crystal powders of $Cu(paz\cdot(COO)_2)$ show a symmetric PMR curve with a low-field shift as shown in Fig. 3. The shift and the peak-to-peak width are plotted against temperature in Fig. 4. The observed curve can be decomposed into two simple derivative curves with the same intensity and width. The separation between the centers of the two components is practically independent of temperature as shown in Fig. 4. This suggests that the structure of the observed curve is due to dipole–dipole interaction between neighboring protons in the ligand. Polycrystalline materials containing close pairs of protons show a double-peaked PMR absorption curve with a separation approximated by [11]

$$\delta H = 3\mu_p/r^3 \quad (1)$$

where μ_p denotes the magnetic moment of a proton and r is the distance between neighboring protons. Polycrystalline $Cu(NO_3)_2(paz)$ powders show a double-peaked absorption curve attributable to neighboring protons in pyrazine with δH equal to 2.6

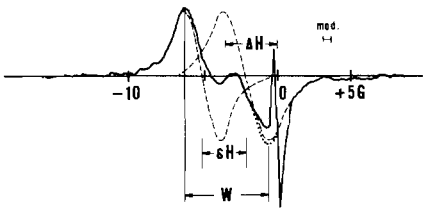

Figure 3. PMR spectrum of polycrystalline pyrazine-2,3-dicarboxylatocopper(II) observed at 40 MHz and 109 K. The sharp component at the origin is due to isohexane employed as an external standard.

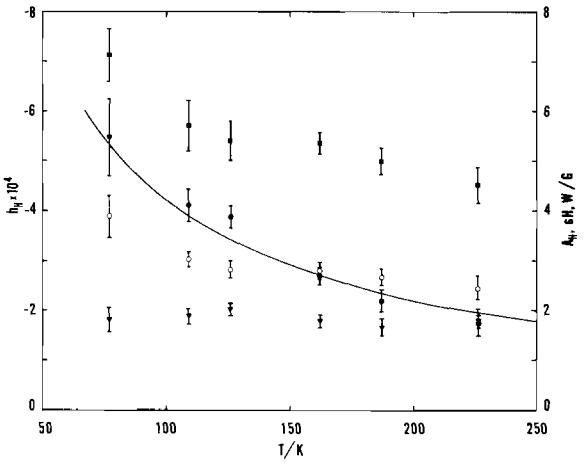

Figure 4. Temperature dependence of the shift $h_H = \Delta H_H/H_0$ (•), the hyperfine coupling constant A_H (▾), the separation between the centers of the component curves δH (○), and the peak-to-peak width W (▪) observed for $Cu(paz\cdot(COO)_2)$. The solid curve represents the shift calculated with the average coupling constant.

G [6]. The separation, δH = 2.8 G, of Cu(paz·$(COO)_2$) yields 2.5 Å for the shortest interproton distance, which agrees well with 2.42 Å in the pyrazine complex [6, 8]. Thus, the structure in the spectrum of the pyrazine-2,3-dicarboxylate is interpreted in terms of the interproton interaction. This shows that all protons involved in the complex are equivalent to one another, supporting the structure illustrated in Fig. 2.

The shifts is ascribable to the paramagnetic property, because it depends on temperature proportionally to the magnetic susceptibility. Generally, a paramagnetic shift arises from the Fermi contact interaction, dipolar interaction between proton and electron moments, and a dipole field from unpaired electrons localized on paramagnetic ions. The last two anisotropic terms make a negligibly small contribution to paramagnetic shifts in polycrystalline powders of copper(II) complexes [6, 8]. Hence, the observed shift is attributable to the contact term given by [8, 12]

$$h_i = \Delta H_i/H_0 = -A_i\chi/Ng_N\mu_N \qquad (2)$$

By use of this equation, the hyperfine coupling constant A_i (in Gauss) can be evaluated from the shift observed at each temperature on the basis of the magnetic susceptibility χ reported by Matthews and Walton [5]. The coupling constant obtained is practically temperature independent (Fig. 4), the average value being equal to 1.78 G. The solid curve in Fig. 4 shows the shift calculated by equation (2) with the average coupling constant.

The hyperfine coupling constant of a proton is proportional to spin density ρ_C on a carbon atom bonded to the proton [12]:

$$A_H = Q_C^H \rho_C \qquad (3)$$

Here, Q_C^H is a proportionality constant equal to −23.7 G for >ĊH species of nitrogen heterocycles [7]. Spin density on the carbon atoms of pyrazine rings is evaluated as ρ_C = −0.07, in good agreement with −0.07–−0.08 in $Cu(NO_3)_2$(paz) [6, 8].

PMR Spectrum of $Cu(NO_3)_2$(2,5-dmpaz)

Figure 5A shows a typical PMR absorption derivative curve observed for the crystal powders of $Cu(NO_3)_2$(2,5-dmpaz). A sharp component at ΔH = 0 in the curve is due to isohexane employed as an external standard. The intrinsic curve can be resolved into two simple derivative curves of intensity ratio equal to 3:1 (broken curves in Fig. 5A). From the intensity ratio, the stronger component shifted to a high field can be assigned to methyl protons and the weaker one shifted to a low field is attributable to protons in pyrazine rings. The shift of each component is plotted against temperature in Fig. 6. The absolute shifts increase with decreasing temperature, indicating that the shifts arise from the paramagnetic

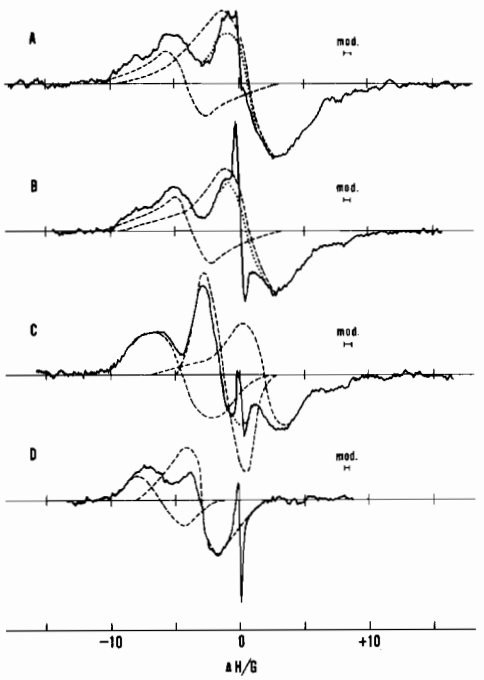

Figure 5. Broad-line PMR spectra of (A) $Cu(NO_3)_2$(2,5-dmpaz) observed at 109 K, (B) $Cu(NO_3)_2$(2,6-dmpaz) at 105 K, (C) $Cu(NO_3)_2$(qux) at 106 K, and (D) $Cu(NO_3)_2$(Cl-paz) at 107 K. The sharp component at ΔH = 0 in each spectrum is due to isohexane employed as an external standard. Each intrinsic signal can be resolved into component curves drawn by broken curves. The dotted curve in each spectrum shows the superposition of the component curves.

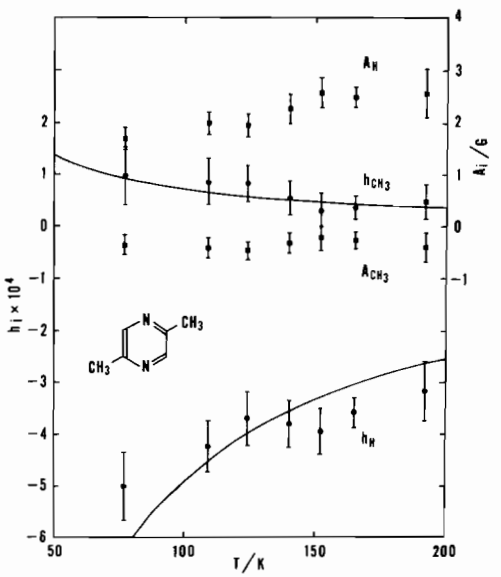

Figure 6. Shifts h_i and contact coupling constants A_i of $Cu(NO_3)_2$(2,5-dmpaz). The solid curves show shifts calculated with the average values of the corresponding coupling constants.

TABLE I. g Factors $g_{\parallel}$ and $g_{\perp}$ (at Room Temperature), Contact Coupling Constant A_i, and Spin Density ρ_C on Carbon Atoms.

Compound	$g_{\parallel}$	$g_{\perp}$		A_i/G	ρ_C
$Cu(NO_3)_2$(2,5-dmpaz)	2.266	2.058	CH	2.2_3	−0.09
			CCH_3	-0.3_3	−0.01
$Cu(NO_3)_2$(2,6-dmpaz)	2.267[a]	2.062[a]	CH	$\sim 1.9_7$[b]	~ −0.08[b]
			CCH_3	-0.3_7	−0.01
$Cu(NO_3)_2$(qux)	2.297[c]	2.041[c]	C(a)H	2.4_1	−0.10
			C(b)H	-0.8_4	0.04
			C(c)H	0.7_6	−0.03
$Cu(NO_3)_2$(Cl-paz)	2.279	2.061	C(a)H	2.4_9	−0.11
			C(b,c)H	1.2_2	−0.05
$Cu(NO_3)_2$(paz)	2.276[d]	2.055[d]	CH	1.9[e]	−0.08[e]
Cu(paz·$(COO)_2$)	2.251	2.045	CH	1.7_8	−0.07

[a]The g factors are temperature dependent: $g_{\parallel} = 2.275$ and $g_{\perp} = 2.056$ at 87 K. [b]The values are temperature dependent. [c]The ESR pattern is the same as that reported in ref. 9, but the g factors are different owing to the different procedures of the analyses. [d]The g factors are determined as $g_z = 2.2714$, $g_y = 2.0669$, and $g_x = 2.0543$ for a single crystal (R. J. Dudley, R. J. Fereday, B. J. Hathaway, P. G. Hodgson, and P. C. Power, *J. Chem. Soc. Dalton*, 1044 (1973)). [e]Ref. 6.

effects. The exchange integral and the g value were determined from the magnetic susceptibility measured down to liquid helium temperature [4]. The contact coupling constant of each component curve can be evaluated from the observed shift and the magnetic susceptibility calculated by the high-temperature expansion method [13] with the magnetic parameters reported already [4]. The curves in Fig. 6 are calculated from equation (2) with the corresponding average values of A_i, reproducing well the observed shifts. The average value of A_i leads to the spin density $\rho_C = -0.09$ on a carbon atom bonded to the resonant proton. When a methyl group undergoes a free rotation, the coupling constant of the methyl protons is proportional to the π-electron spin density on a carbon atom attached to the methyl group:

$$A_{CH_3} = Q_C^{CH_3}\rho_C \qquad (4)$$

The proportionality constant $Q_C^{CH_3}$ is usually assumed to be equal to +29.3 G [14]. From the average A_{CH_3} value, spin density on a carbon atom attached to the methyl group can be evaluated to be equal to −0.01. Its absolute value is much smaller than that of spin density on the carbon atoms of unsubstituted pyrazine in $Cu(NO_3)_2$(paz). This arises from the inductive effect of methyl groups. All carbon atoms in the pyrazine rings of $Cu(NO_3)_2$(2,5-dmpaz) carry negative spin densities as in $Cu(NO_3)_2$(paz). This suggests that a positive spin density is distributed on nitrogen atoms [6, 8].

PMR Spectrum of $Cu(NO_3)_2$(qux)

The PMR curve of $Cu(NO_3)_2$(qux) consists of three component curves of almost the same intensity (Fig. 5C). This indicates that three kinds of CH species in a quinoxaline molecule carry spin densities different from each other. Nitrogen atoms bonded to copper are presumed to carry a positive spin density in accordance with the results for $Cu(NO_3)_2$(paz) and $Cu(NO_3)_2$(2,5-dmpaz). Hence, spin densities on the carbon atoms C(a) and C(c) (see the chemical formula in Fig. 7) are negative in sign and that of C(b) is positive, because spin delocalization through π electron systems bears alternation in sign of spin density [10]. Thus, the component curve shifted to a

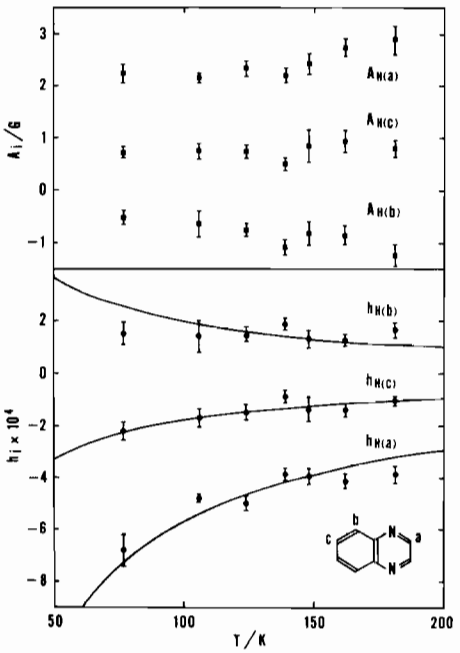

Figure 7. Shifts h_i and contact coupling constants A_i of $Cu(NO_3)_2$(qux). The solid curves show shifts calculated with the corresponding average coupling constants listed in Table I.

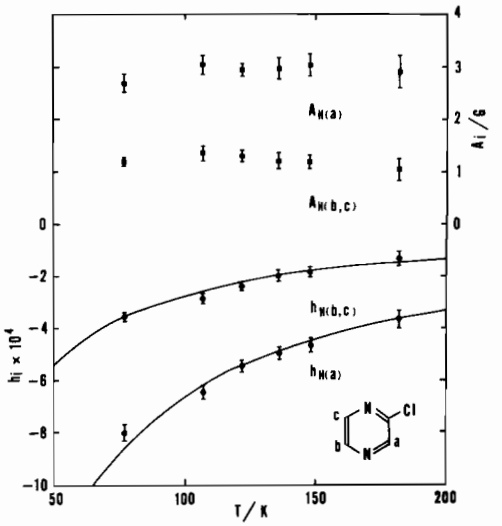

Figure 8. Shifts h_i and contact coupling constants A_i of $Cu(NO_3)_2$(Cl-paz). The solid curves show shifts calculated with the corresponding coupling constants listed in Table I.

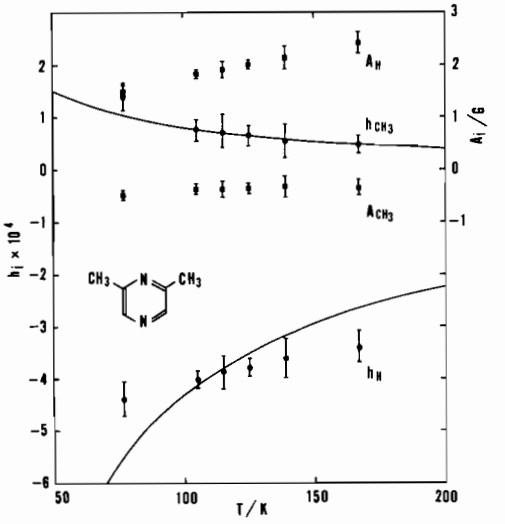

Figure 9. Shifts h_i and contact coupling constants A_i of $Cu(NO_3)_2$(2,6-dmpaz). The solid curves show shifts calculated with the corresponding coupling constants listed in Table I.

high field can be assigned to protons attached to C(b) atoms. The positive spins delocalized from copper to a nitrogen atom strongly polarize the $p\pi$ orbitals of carbon atoms existing at the either side of the nitrogen atom. Accordingly, the component curve of the largest coupling constant is attributable to the protons of C(a)H species. One of the three component curves has a sharper peak-to-peak width than those of others. This suggests that the protons presenting the sharp curve are distant from paramagnetic ions: the curve can be assigned to C(c)H protons in conformity with the above assignment. Figure 7 shows that the shifts are reproduced well with the solid curves calculated by use of equation (2) with the corresponding coupling constants cited in Table I.

PMR Spectrum of $Cu(NO_3)_2$(Cl-paz)

The PMR spectrum consists of two components of intensity ratio equal to 2:1 (Fig. 5D). Because the spin densities on the carbon atoms C(b) and C(c) (Fig. 8) are expected to be nearly equal to each other, the stronger component curve is attributable to the protons of C(b)H and C(c)H species, and the weaker one shifted to a greater extent is to C(a)H protons. Table I shows the average coupling constants and the spin densities on the carbon atoms. The carbon atom C(a) carries a negative spin to a greater extent than C(b) and C(c) atoms. This can be explained by a flow of electronic charge from chlorine atoms to pyrazine rings.

PMR Spectrum of $Cu(NO_3)_2$ (2,6-dmpaz)

The intrinsic PMR spectrum of $Cu(NO_3)_2$ (2,6-dmpaz) is made up of two component curves of intensity ratio equal to 3:1 (Fig. 5B). The stronger component is attributable to methyl protons and the weaker one to protons of pyrazine rings. The solid curves in Fig. 9 show h_{CH_3} and h_H calculated with the coupling constants −0.37 and 1.97 G, respectively. The shift h_H deviates systematically from the curve calculated, and so A_H decreases, as temperature lowers.

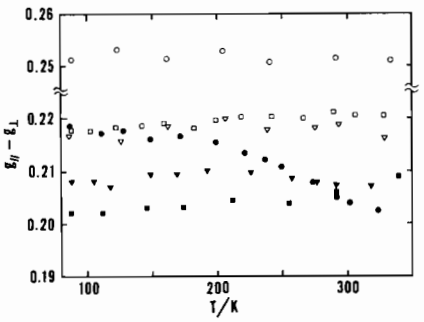

Figure 10. Temperature dependence of the g anisotropy, $g_\parallel - g_\perp$. ▼: $Cu(NO_3)_2$ (2,5-dmpaz), ●: $Cu(NO_3)_2$(2,6-dmpaz), ○: $Cu(NO_3)_2$(qux), ▽: $Cu(NO_3)_2$(Cl-paz), □: $Cu(NO_3)_2$(paz), ■: Cu(paz·$(COO)_2$).

ESR Spectra

The crystal powders of each complex show an ESR spectrum characteristic of d^9 complexes having an axial ligand field. No hyperfine structure due to copper was observed in any spectrum. The g factors determined are listed in Table I. The spectrum of $Cu(NO_3)_2$(qux) is broad compared with those of other complexes so that the g factors of the qux complex have a large uncertainty. The g anisotropy

$g_\parallel - g_\perp$ of $Cu(NO_3)_2$ (2,6-dmpaz) is temperature dependent as seen in Fig. 10, although the spectrum exhibits the same pattern over the temperature range investigated. The $g_\parallel - g_\perp$ values of other complexes are substantially temperature independent.

To a first approximation, the following equations are derived for the ground wave functions of a copper(II) ion carrying an unpaired electron in its $d_{x^2-y^2}$ orbital:

$$\phi^+ = d_{x^2-y^2}{}^+ + ic_1 d_{xy}{}^+ + c_2(d_{xz}{}^- - id_{yz}{}^-)/2, \quad (5)$$

$$\phi^- = d_{x^2-y^2}{}^- - ic_1 d_{xy}{}^- - c_2(d_{xz}{}^+ - id_{yz}{}^+)/2, \quad (6)$$

where + and − denote positive and negative spins, respectively, and x, y, and z axes are defined as shown in Figs. 1 and 2.

The g factors of the copper(II) ion are given by [15]

$$g_\parallel = 2 + 8c_1, \quad (7)$$

$$g_\perp = 2 + 2c_2, \quad (8)$$

These equations are consistent with the relation, $g_\parallel > g_\perp > 2$, observed for every complex studied.

Discussion

A negative spin density is distributed in the $p\pi$ orbitals of carbon atoms bonded to nitrogen atoms in every complex subject to the present PMR study. This suggests that an unpaired electron of a copper atom induces a positive spin density in the $p\pi$ orbitals of nitrogen atoms bonded to the copper atom. For the spin delocalization from copper to ligand molecules, the following mechanisms are conceivable:

(A) $d_{x^2-y^2}$(Cu)α——$p\sigma$(N)α- - -$p\pi$(N)α——$p\pi$(C)β

(B) $d_{x^2-y^2}$(Cu)α- - -d_{xz}(Cu)β——$p\pi$(N)α——$p\pi$(C)β

(C) $d_{x^2-y^2}$(Cu)α- - -d_{xy}(Cu)α——$p\pi$(N)β——$p\pi$(C)α

(D) $d_{x^2-y^2}$(Cu)α——$p\pi$(C)β

Here, α and β denote respectively excess positive and negative spins localized in the orbitals, the solid lines show bond formation between neighboring atoms, and the broken lines represent orbital mixing within an atom in question. Figure 11 shows mechanism (A) schematically; the $d_{x^2-y^2}$ orbital of a copper(II) ion correlates to the lone-pair orbitals of nitrogen atoms bonded to the copper atom, inducing a fractional positive spin in the lone-pair orbitals. It successively creates a spin density of the same sign on the nitrogen p_z orbital through $p\sigma$–$p\pi$ interaction, because the two nitrogen orbitals are orthogonal to

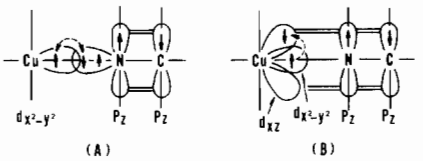

Figure 11. Mechanisms of spin delocalization from copper(II) ions to the π system of ligand molecules: mechanism (A) through $d\sigma$–$p\sigma$ bonding and mechanism (B) through $d\pi$–$p\pi$ bonding.

each other. In mechanisms (B) and (C), the spin–orbit coupling of copper plays an important role. The ground wave function with α spin is given by equation (5): d_{xz} carries a β spin density and d_{xy} does an α spin density. Mechanism (B) is illustrated in Fig. 11B: a fractional β spin of d_{xz} yields a positive spin density in $p\pi$(N). Another type of π delocalization is given by mechanism (C). It induces a spin density distribution opposed to that due to mechanism (B): the positive spin density of d_{xy} yields a negative spin density in $p\pi$(N). In $Cu(NO_3)_2$·(paz), the plane of pyrazine molecules is tilted out of the CuN_2O_2 plane [1]. Hence, unpaired electrons of $d_{x^2-y^2}$ are capable of diffusing into the carbon atoms of pyrazine rings through the direct overlap of $d_{x^2-y^2}$ with the carbon $p\pi$ orbitals. Richardson and Hatfield [4] proposed this type of mechanism, *i.e.*, mechanism (D), for the spin delocalization in the $Cu(NO_3)_2L$ type complexes.

Mechanisms (C) and (D) are ruled out for Cu(paz·$(COO)_2$), because the plane of the heterocyclic rings is parallel to the CuN_2O_2 plane. The relative strength of the $p\sigma$–$p\pi$ interaction and the $d_{x^2-y^2}$–d_{xz} mixing gives a measure of contributions from mechanisms (A) and (B). The magnitude of the former can be estimated from hyperfine splittings due to nitrogen in the ESR spectra of organic radicals. For a C–N–C fragment having π electrons on it, a hyperfine coupling constant A_N due to the nitrogen nucleus is given by [16]

$$A_N = Q_N^N \rho_N = Q_{NN}^N \rho_N + 2Q_{CC}^N \rho_N. \quad (9)$$

This originates from the $p\sigma$–$p\pi$ interaction: a spin density is created in the sp^2 orbitals of nitrogen by configuration interaction between the ground state configuration and a singly excited one involving a σ–σ^* excitation. The proportionality constants have been determined as Q_{NN}^N = 19.1 G and Q_{CC}^N = 9.1 G [16]. Q_{NN}^N gives a measure for the spin polarization of nitrogen s electrons. Because the coupling constant for an electron localized in a pure nitrogen s orbital is equal to 557 G [15], the ratio 19.1/557 (= 0.03) gives a measure of the $p\sigma$–$p\pi$ interaction. The $d_{x^2-y^2}$–d_{xz} mixing coefficient c_2 in equation (5) is evaluated to be equal to 0.02 from the observed $g_\perp$ factor with equation (8). These imply

that the $p\sigma$–$p\pi$ and $d_{x^2-y^2}$–d_{xz} interactions are of the same order of magnitude. The overlap between $d_{x^2-y^2}$ and the lone-pair orbitals is expected to be larger than that between d_{xz} and p_z. Therefore, mechanism (A) is thought to contribute to the spin delocalization to a greater extent than mechanism (B).

In $Cu(NO_3)_2L$ type complexes also, mechanism (A) is probably predominant in spin delocalization, since the above deduction holds for the complexes. In the spin delocalization of the complexes, however, mechanisms (C) and (D) are operative in addition to mechanisms (A) and (B), because the plane of the pyrazine rings is tilted out of the CuN_2O_2 plane. The relative magnitude of the contributions from mechanisms (B) and (C) can be estimated from the orbital-mixing coefficients in equation (5): c_1 shows the magnitude of $d_{x^2-y^2}$–d_{xy} interaction, and c_2 that of $d_{x^2-y^2}$–d_{xz} interaction. The coefficients are related to g factors given by equations (7) and (8). The temperature-dependent g anisotropy of $Cu(NO_3)_2$ (2,6-dmpaz) shows that c_1 increases and c_2 decreases with decreasing temperature: the contribution from mechanism (C) increases and that from mechanism (B) decreases as the temperature lowers. The former yields a positive spin density on the carbon atoms, whereas the latter does a negative spin density. Therefore, the magnitude of the negative spin density localized on the carbon atoms is reduced with lowering temperature, explaining well the temperature dependence of A_H in the 2,6-dmpaz complex. This gives evidence to the contribution of mechanisms (B) and (C) to the spin delocalization. The A_{CH_3} value also must be temperature dependent, but it shows no appreciable temperature dependence. Probably, the absolute value is so small that the effect does not appear extensively. Other complexes show no marked temperature dependence of the g anisotropy, consistent with the fact that the A_H values are practically temperature-independent. The temperature-dependent $g_\parallel - g_\perp$ and A_H observed solely for $Cu(NO_3)_2$ (2,6-dmpaz) arise probably from a large steric effect due to methyl groups at the positions 2 and 6. The effect may be a dominant factor to the tilt angle between the pyrazine-ring and CuN_2O_2 planes. When the motion of the methyl groups is thermally activated, the tilt angle can be changed for the steric requirement. This gives rise to a change of the ratio c_1/c_2 and, hence, that of the relative magnitude in the contribution of mechanisms (B) and (C).

Recent magnetic resonance studies [17] carried out on $R_2[CuCl_4(H_2O)_2]$ indicated that a fractional spin amounting to 0.4 is delocalized from copper to the ligands and each oxygen atom carries a spin density equal to 0.07. This provides a convincing example showing that the magnitude of spin delocalization is an important factor in superexchange interaction. However, the strength of the Cu–O covalent bonding shows no appreciable relation to that of the exchange interaction. For the complexes subject to the present study also, neither the spin density nor the g factor shows appreciable relation to the exchange integral. The results obtained, however, have indicated that all of mechanisms (A), (B), and (C) are operative as described above. Richardson and Hatfield [4] showed a relation between the exchange integral and the π–π^* transition energy of the heterocyclic ligands in the series of complexes, and proposed mechanism (D). Probably, the superexchange interaction arises from a complicatedly combined effect of the four mechanisms proposed.

References

1 A. Santro, A. A. Mighell, and C. W. Reimann, *Acta Crystallogr. Ser. B, 26,* 979 (1970).
2 J. C. Bonner and M. E. Fisher, *Phys. Rev., 135,* A640 (1964).
3 D. B. Losee, H. W. Richardson, and W. E. Hatfield, *J. Chem. Phys., 59,* 3600 (1973).
4 H. W. Richardson and W. E. Hatfield, *J. Am. Chem. Soc., 98,* 835 (1976).
5 R. W. Matthews and R. A. Walton, *Inorg. Chem., 10,* 1433 (1971).
6 M. Inoue, S. Emori, K. Hara, and M. Kubo, *J. Magn. Resonan., 17,* 212 (1975).
7 M. Inoue and M. Kubo, *Coord. Chem. Rev., 21,* 1 (1976).
8 M. Inoue, *J. Magn. Resonan., 27,* 159 (1977).
9 H. W. Richardson, W. E. Hatfield, H. J. Stoklosa, and J. R. Wasson, *Inorg. Chem., 12,* 2051 (1973).
10 M. Inoue, H. Kuramoto, and D. Nakamura, *Bull. Chem. Soc. Jpn., 50,* 2885 (1977).
11 E. R. Andrew, "Nuclear Magnetic Resonance", Cambridge Univ. Press, London (1955) p. 152.
12 G. N. LaMar, D. De W. Horrocks, Jr., and R. H. Holm (eds.), "NMR of Paramagnetic Resonance", Academic Press, New York and London (1973).
13 G. S. Rushbrooke and P. J. Wodd, *Mol. Phys., 1,* 257 (1958).
14 E. T. Kaiser and L. Kevan (eds.), "Radical Ions", Interscience Publishers, New York (1968) pp. 20, 182.
15 B. A. Goodman and J. B. Rayner, *Adv. Inorg. Chem. Radiochem., 13,* 135 (1970).
16 J. C. M. Henning, *J. Chem. Phys., 44,* 2139 (1966).
17 W. J. Looyestijn, T. O. Klaassen, and N. J. Poulis, *Physica, 93B,* 349 (1978).